Spleen tyrosine kinase-induced JNK-dependent NLRP3 activation is involved in diabetic cardiomyopathy

SHENGYU LI[1*], RUIQING LIU[1*], MEITING XUE[1*], YINGCHUN QIAO[1,2], YUFENG CHEN[1], GUANGFENG LONG[1], XIXI TIAN[1], YAHUI HU[1], PENGFEI ZHOU[1], XIAOHUI DONG[1], ZHI QI[3,4], YUJIE CUI[1,5] and YANNA SHEN[1]

[1]School of Medical Laboratory, [2]Tianjin Metabolic Diseases Hospital, Tianjin Medical University, Tianjin 300203; [3]Department of Histology and Embryology, School of Medicine, Nankai University, Tianjin 300071; [4]National Clinical Research Center of Kidney Diseases, Beijing 100853; [5]The Key Laboratory of Myocardial Ischemia, Harbin Medical University, Ministry of Education, Harbin, Heilongjiang 150086, P.R. China

Received October 8, 2018; Accepted March 20, 2019

DOI: 10.3892/ijmm.2019.4148

Abstract. Diabetic cardiomyopathy (DCM) is a leading contributor to the increased morbidity and mortality rates associated with diabetes. Persistent inflammation has previously been reported to be involved in the pathogenesis of DCM. However, the exact underlying molecular mechanisms remain to be fully elucidated. In the present study, the role of spleen tyrosine kinase (Syk) and c-Jun N-terminal kinase (JNK) in NLR family pyrin domain-containing 3 (NLRP3 inflammasome) activation in DCM were investigated *in vivo* and *in vitro*. Streptozotocin (65 mg/kg) was injected intraperitoneally into Sprague-Dawley rats to induce a rat model of diabetes. Neonatal rat cardiomyocytes and H9c2 cells were cultured to detect the expression of JNK, NLRP3 and its associated downstream molecules, following treatment with Syk/JNK inhibitor or Syk/JNK-small interfering (si)RNA in high glucose (HG) conditions. It was revealed that the protein and mRNA expression levels of phospho (p)-Syk, p-JNK, NLRP3 and its associated downstream molecules, including interleukin (IL)-1β, were upregulated *in vivo* and *in vitro*. The JNK inhibitor significantly decreased the expression of NLRP3 and its downstream molecules in neonatal rat cardiomyocytes and H9c2 cells treated with HG. Furthermore, Syk-siRNA and the Syk inhibitor markedly inhibited the HG-induced activation of JNK, followed by the downregulation of NLRP3 and its downstream molecules at the mRNA and protein levels in cells. Therefore, it was demonstrated that the HG-induced activation of NLRP3 was mediated by the activation of Syk/JNK, which subsequently increased the protein expression levels of mature IL-1β, suggesting that the Syk/JNK/NLRP3 signaling pathway serves a critical role in the pathogenesis of DCM.

Correspondence to: Professor Yujie Cui or Professor Yanna Shen, School of Medical Laboratory, Tianjin Medical University, 1 Guangdong Road, Hexi, Tianjin 300203, P.R. China
E-mail: yujiecui1@126.com
E-mail: shenyanna@sina.com

*Contributed equally

Key words: diabetic cardiomyopathy, spleen tyrosine kinase, c-Jun N-terminal kinase, NLR family pyrin domain-containing 3 inflammasome, interleukin-1β

Introduction

Diabetic cardiomyopathy (DCM) is currently defined as a cardiac disease independent of vascular complications during diabetes, which is the foremost contributor to the increased rates of morbidity and mortality in patients with diabetes. The International Diabetes Federation estimated a worldwide rise in the prevalence of diabetes mellitus (DM) to 552,000,000 by 2030 (1). The prevalence of DCM in the diabetic population is 20-60%, affecting patients with type 1 and 2 DM (2,3). Furthermore, the relative risk of developing heart failure in patients with diabetes is between 2- and 3-fold higher compared with that in the general population (4). Hyperglycemia-induced persistent inflammation and oxidative stress, resulting in interstitial fibrosis, contractile dysfunction and dysfunctional remodeling, have previously been confirmed as high risk factors for the pathogenesis and progression of DCM (2,5,6). However, how high glucose (HG) leads to the extensive and uncontrollable expression of pro-inflammatory mediators, which cause widespread inflammation and tissue dysfunction in the pathogenesis of DCM, remains to be fully elucidated.

Extensive evidence suggests that interleukin (IL)-1β serves a vital role in the progression of cardiac inflammation, fibrosis, cell apoptosis and cardiac dysfunction (7-10). A previous study showed that serum IL-1β promoted endoplasmic reticulum stress-induced myocyte apoptosis in DCM via IL-1 receptor-associated kinase-2 (8). Another study showed that IL-1β was involved in the early inflammatory phase of human diabetic cardiovascular disease (7). Westermann *et al* demonstrated that excessive accumulation of collagen fibers in the cardiac interstitium was associated with increased IL-1β and transforming growth factor-β in DCM (9). Consistently, a recent study reported that HG induced collagen synthesis by increasing the production of IL-18 and IL-1β in cardiac

fibroblasts (10). Previous studies have demonstrated that a caspase-1-activating protein complex, termed the NLR family pyrin domain-containing 3 (NLRP3) inflammasome, is assembled to induce the activation of caspase-1, producing cleaved caspase-1 p20, known as p20, leading to the maturation and secretion of IL-1β in type 1 and 2 DM (11-13). Luo *et al* (14) reported that the NLRP3 inflammasome regulates the death of cardiomyocytes and the activation of fibroblasts in DCM, which is involved in the structural and functional disorder of DCM. Further investigations examining the regulatory mechanisms and upstream molecules of NLRP3 inflammasome activation in DCM are required.

Spleen tyrosine kinase (Syk), a cytoplasmic protein tyrosine kinase, is known to mediate innate immune recognition and have the ability to specifically regulate the function of diabetogenic T cells in type 1 DM (15). c-Jun N-terminal kinase (JNK) belongs to the mitogen-activated protein kinase (MAPK) family, and is involved in influencing the signaling of cardiac development, metabolism, performance and pathogenesis (16). Previous studies have identified JNK as a key transcriptional regulator of inflammation, which is activated in response to inflammatory cytokines and oxidative stress under HG conditions (17,18). Watanabe *et al* (19) reported that the MAPK family, including extracellular signal-regulated kinases (ERKs), p38 and JNK, is involved in the development of diabetic nephropathy. Furthermore, the phosphorylation of Syk can lead to the activation of ERK and subsequently activate nuclear factor (NF)-κB in diabetic nephropathy (20).

Based on the above findings, it was hypothesized that JNK, Syk and NLRP3, in addition to its associated downstream molecules, serve indispensable roles in the development of DCM. In the present study, it was demonstrated that the HG-induced activation of NLRP3 is mediated by the activation of Syk/JNK and subsequently increases the protein expression level of mature (m)IL-1β. This suggests that the Syk/JNK/NLRP3 signaling pathway serves a critical role in the pathogenesis of DCM.

Materials and methods

Reagents and antibodies. Glucose, mannitol (Mtol) and streptozotocin (STZ) were purchased from Sigma-Aldrich; Merck KGaA (Darmstadt, Germany). JNK inhibitor II SP600125 (SP) was purchased from Merck KGaA, Syk inhibitor IV, BAY61-3606 was purchased from Santa Cruz Biotechnology, Inc. (Dallas, TX, USA) and TRIzol® reagent was purchased from Invitrogen (Thermo Fisher Scientific, Inc., Waltham, MA, USA). Antibodies for phospho (p)-JNK (p-JNK, cat. no. 9255s, 1:1,000), JNK (cat. no. 9252s, 1:1,000), p-Syk (cat. no. 2710s, 1:1,000), Syk (cat. no. 13198s, 1:1,000), NLRP3 (cat. no. 13158s, 1:1,000) and cleaved caspase-1 p20 (cat. no. 4199, 1:1,000) were purchased from Cell Signaling Technology, Inc. (Danvers, MA, USA). Antibodies for caspase-1 (cat. no. ab179515, 1:1,500), pro-IL-1β (cat. no. ab2105, 1: 2,000) and mIL-1β (cat. no. ab9722, 1:2,000) were purchased from Abcam (Cambridge, UK). The antibody for β-actin (cat. no. sc-47778, 1:1,000) was purchased from Santa Cruz Biotechnology, Inc., and antibodies for anti-mouse immunoglobulin G (IgG) HRP conjugate (cat. no. W4021, 1:5,000) and anti-rabbit IgG HRP conjugate (cat. no. W4011, 1:5,000) were purchased from Promega Corporation (Madison, WI, USA).

Animal care and STZ-induced diabetic rat models. A total of 60 male Sprague-Dawley rats (age, 5 weeks; weight, 180-220 g) were purchased from the Laboratory Animal Center of the Academy of Military Medical Sciences (Beijing, China). All rats were housed in standard conditions of temperature (22±4˚C) and humidity (60±5%) with an alternating 12-h light/dark cycle. Clean drinking water and a standard pellet diet were available. The rats were randomly divided into a control group (n=24) and a diabetes groups (n=36). The rats in the diabetic group (n=36) were treated with a single intraperitoneal injection (i.p.) of fresh STZ (65 mg/kg in citrate buffer 0.1 mol/l, pH 4.5), whereas the rats in the control group (n=24) received the same volume of sodium citrate buffer. The blood glucose level was measured with a portable glucometer (UltraEasy; Johnson & Johnson, New Brunswick, NJ, USA) on days 3 and 7 following STZ or sodium citrate buffer injection. Rats with a random blood glucose level of >16.7 mM in two consecutive tests were considered diabetic. Body weight and blood glucose levels were monitored twice a week. Cardiac function was measured at 12 weeks, as described in our previous study (21). A total of 13 rats (seven rats from the diabetes group and six rats from the control group) were sacrificed by cervical dislocation under anesthesia (single intraperitoneal injection of 10% chloral hydrate at the dose of 350 mg/kg body weight) at 12, 16, 20 and 33 weeks, respectively. The hearts were then harvested and all tissue samples were subjected to mRNA and protein expression analyses. All efforts were made to minimize suffering. All experimental procedures in the present study were approved by the Animal Care and Welfare Committee of Tianjin Medical University (Tianjin, China).

Cardiac function measurements by echocardiography. To assess cardiac function, transthoracic echocardiography was performed in rats using the Vivid 3 Pro imaging system (GE Healthcare, Chicago, IL, USA). Imaging was performed on the control and diabetes group rats following light anesthesia with 3% inhaled isoflurane at 12 weeks. The derived echocardiography parameters were the average of six consecutive cardiac cycles. The measured indices included left ventricular fractional shortening (FS%), left ventricular ejection fraction (EF%) and peak E to peak A ratio (E/A). The directly measured indices included left ventricle (LV) internal dimension (LVID) in diastole (LVID,d) and systole (LVID,s), LV posterior wall thickness in diastole and systole, and interventricular septal thickness during diastole (IVS, d) and systole (IVS, s). The percentage of LV shortening fraction (FS) = [(LVID,d - LVID,s)/LVID,d] x100; LV ejection fraction (EF) percentage = [(LV end-diastolic volume-LV end-systolic volume)/LV end-diastolic volume] x100.

Isolation and culture of neonatal cardiomyocytes. Neonatal rat cardiomyocytes were obtained from the hearts of 200 neonatal Sprague-Dawley rats (within 48 h of birth), which were generated via mating, 24 female rats and 8 male rats (Laboratory Animal Center of the Academy of Military Medical Sciences, Beijing, China). All animal procedures were approved by the

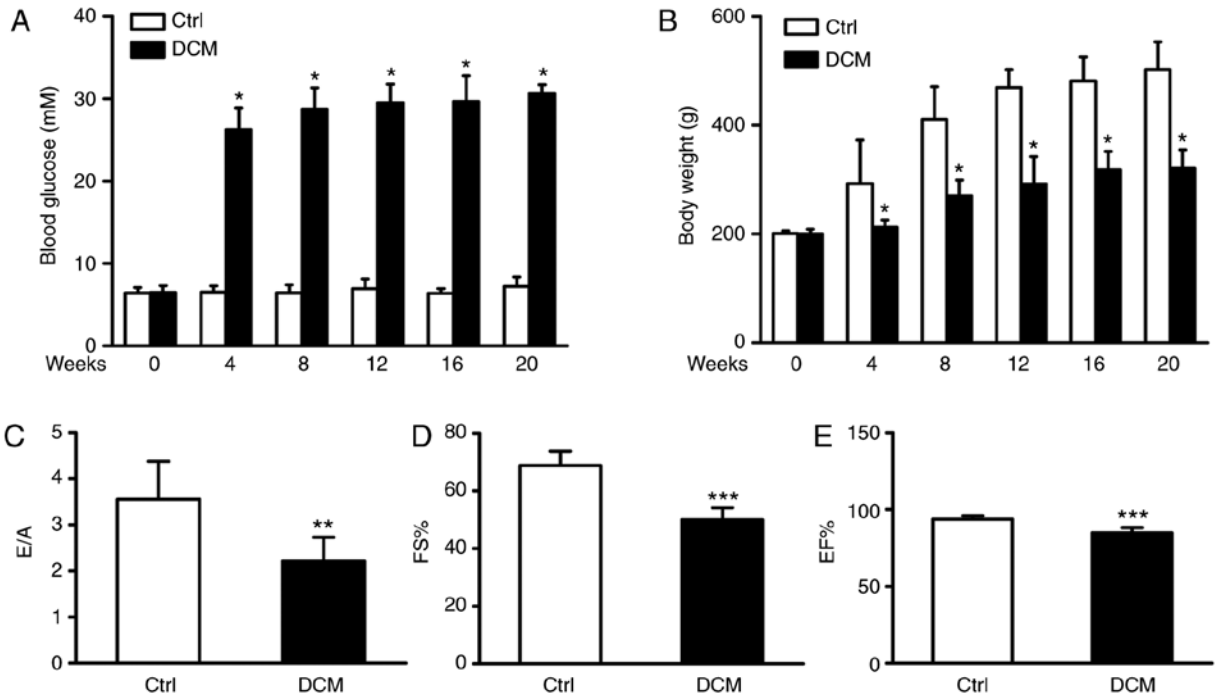

Figure 1. General characteristics of DCM and Ctrl rats. (A) Random blood glucose levels in Ctrl (n=24) and DCM (n=36) groups. (B) Body weights in the Ctrl (n=24) and DCM (n=36) groups. Echocardiography performed on rat hearts from the Ctrl (n=5) and DCM (n=10) groups at 12 weeks. (C) E/A, (D) FS% and (E) Left ventricular EF%. Values are presented as the mean ± standard deviation. *P<0.05, **P<0.01 and ***P<0.001, vs. Ctrl by two-way analysis of variance. DCM, diabetic cardiomyopathy; Ctrl, control; E/A, A peak E peak flow ratio; FS%, fractional shortening; EF%, ejection fraction.

Animal Care and Welfare Committee of Tianjin Medical University. The neonatal rats (6-8 g) were anesthetized by intraperitoneal injection of 10% chloral hydrate (30 mg/kg) and sacrificed by cervical dislocation; a midline incision was made through the sternum and the hearts were gently removed under sterile conditions. The ventricles were cut into 1-1.5-mm^3 sections and digested into a single cell suspension with 0.125% trypsin. The digestion process was repeated seven times and for 7 min each time. The digestion process was terminated when fetal bovine serum (FBS; FBS:trypsin, 1:10; Gibco; Thermo Fisher Scientific, Inc.) was added. In order to collect myocardial cells, the single cell suspension was centrifuged at 201 x g for 8 min at 4˚C and then resuspended with Dulbecco's modified Eagle's medium (DMEM; Gibco; Thermo Fisher Scientific, Inc.) containing 10% FBS. The collected cells were incubated for 1-2 h in DMEM containing 10% FBS to remove non-myocytes, appropriate 5-bromo-2-deoxyuridine (0.1 mM) was added to suppress non-myocardial cell growth, and the cardiomyocytes were then seeded in six-well collagen-coated plates at a density of $1x10^6$ cells/well at 37˚C in a humidified atmosphere of 5% CO_2. Following 24-36 h of culture, the cardiomyocytes were exposed to normal glucose (5.5 mM), HG (25.0 mM), and a high Mtol concentration (5.5 mM glucose + 19.5 mM Mtol) for 10 min, and 12, 24 and 36 h at 37˚C, and then harvested for either western blotting or reverse transcription-quantitative polymerase chain reaction (RT-qPCR) analysis.

Cell culture. In the present study, H9c2 cells were purchased from the Institute of Basic Medical Sciences, Chinese Academy of Medical Sciences (Beijing, China). The H9c2 and neonatal cardiomyocyte cells were maintained in DMEM containing 5.5 mM glucose supplemented with 10%, FBS and 1% streptomycin/penicillin at 37˚C and 5% CO_2. The two cell types were added to a 6-well plate at a density of $1x10^6$ cells/well and treated with or without the JNK inhibitor (SP, 10 μM) for 2 h and the Syk inhibitor (BAY61-3606, 1 μM) for 2 h at 37˚C. They were subsequently exposed to 5.5 or 25.0 mM glucose or the high Mtol concentration for 24 h at 37˚C, and then harvested for either western blotting or RT-qPCR analysis.

RT-qPCR analysis. Total RNA was extracted from the rat hearts, neonatal rat cardiomyocytes or H9c2 cells using TRIzol reagent (Thermo Fisher Scientific, Inc.) according to the manufacturer's protocol, and first-strand cDNA was synthesized using the FastQuant RT kit (Tiangen Biotech Co., Ltd., Beijing, China). The PCR reactions were performed with an initial denaturation at 94˚C for 3 min, followed by 35 cycles at 94˚C for 30 sec, 55/59/60˚C for 30 sec, 72˚C for 1 min and final extension at 72˚C for 5 min. The amplified products were detected using 1.5% agarose gel electrophoresis, following staining with ethidium bromide (0.5 μg/ml) for 40 min at room temperature. The primer sequences used were as follows: NLRP3, forward 5'-AGGGCTCTGTTCATTG-3' and reverse 5'-CTTCACGTCTCGGTTC-3'; caspase-1, forward 5'-TGCCTGGTCTTGTGACTTGGAG-3' and reverse 5'-ATGTCCTGGGAAGAGGTAGAAACG-3'; IL-1β, forward 5'-TGGGATGATGACGACCTGC-3' and reverse 5'-GGAGAATACCACTTGTTGGCTTA-3' reverse, and β-actin, forward 5'-GTTGACATCCGTAAAGACC-3' and reverse 5'-GACTCATCGTACTCCTGCT-3'.

Detection of mRNA levels by RT-qPCR. Total RNA was extracted from H9c2 cells using TRIzol reagent and 1 μg RNA

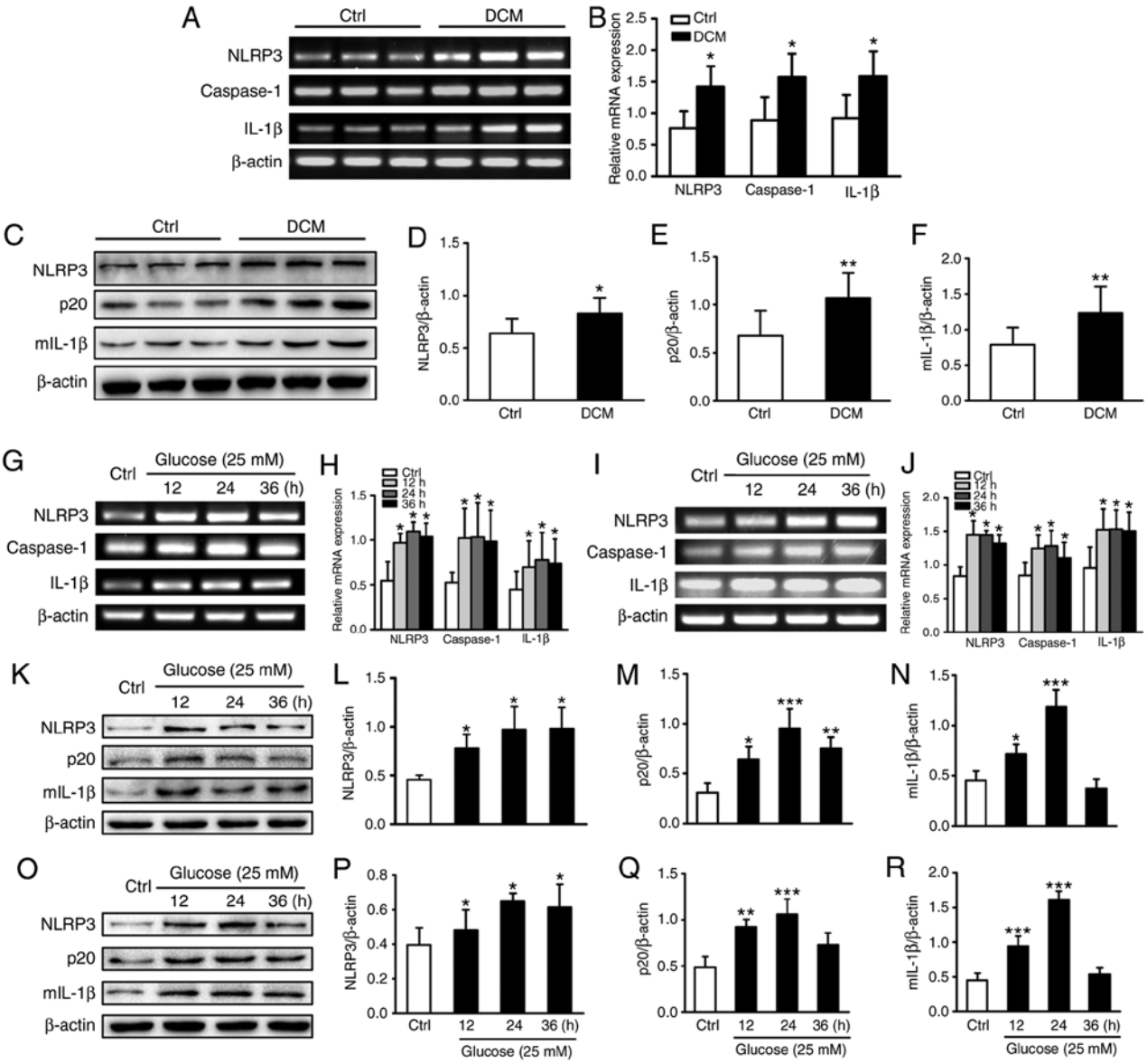

Figure 2. Activation of the NLRP3 inflammasome and phosphorylation of Syk and JNK in the hearts of DCM rats, high glucose-induced H9c2 cells and neonatal cardiomyocytes. (A) Reverse transcription-quantitative polymerase chain reaction analysis of NLRP3, caspase-1 and IL-1β. (B) Quantification of mRNA levels of NLRP3, caspase-1 and IL-1β in rat myocardial tissue (Ctrl, vs. DCM group). (C) Western blotting of NLRP3, p20 and mIL-1β. Relative densitometric quantification analysis of (D) NLRP3, (E) p20 and (F) mIL-1β in C. (G) mRNA expression levels of NLRP3, caspase-1 and IL-1β of H9c2 cells cultured under 5.5 or 25.0 mM glucose conditions for 12, 24 and 36 h. (H) Densitometric analysis of the mRNA expression levels of NLRP3, caspase-1 and IL-1β in H9c2 cells. (I) mRNA expression levels of NLRP3, caspase-1 and IL-1β in neonatal cardiomyocytes. (J) Densitometric analysis of the mRNA expression levels of NLRP3, caspase-1 and IL-1β in neonatal cardiomyocytes. (K) Protein expression levels of NLRP3, p20 and mIL-1β in H9c2 cells cultured under 5.5 or 25.0 mM glucose conditions for 12, 24 and 36 h. Densitometric analysis of the protein expression levels of (L) NLRP3, (M) p20 and (N) mIL-1β H9c2 cells. (O) Protein expression levels of NLRP3, p20 and mIL-1β in neonatal cardiomyocytes. Densitometric analysis of the protein expression levels of (P) NLRP3, (Q) p20 and (R) mIL-1β in neonatal cardiomyocytes. Data are presented as the mean ± standard error of the mean from three independent experiments. Student's t-test was used for comparisons between the Ctrl and DCM groups (B and D-F). One-way analysis of variance followed by Tukey's post hoc test was performed for H, J, L-N and P-R. *P<0.05, **P<0.01 and ***P<0.001, vs. Ctrl group. β-actin was used as the internal loading Ctrl. NLRP3, NLR family pyrin domain-containing 3; Syk, spleen tyrosine kinase; JNK, c-Jun N-terminal kinase; IL, interleukin; Ctrl, control; DCM, diabetic cardiomyopathy; mIL-1β, mature IL-1β; p20, caspase-1 p20.

was reverse transcribed into cDNA using the FastQuant RT kit (Tiangen Biotech Co., Ltd.), according to the manufacturer's protocol. The concentration and integrity of the isolated RNA was measured using NanoDrop (Thermo Fisher Scientific, Inc.). The mRNA levels were analyzed by RT-qPCR using SYBR-Green. The thermocycling conditions were as follows: 95˚C for 30 sec, followed by 40 cycles of 60˚C for 30 sec and 72˚C for 30 sec. RT-qPCR was performed using the Stratagene Mx3005P system (Agilent Technologies, Inc., Santa Clara, CA, USA). The PCR products were analyzed by melting curve using MxPro-Mx3005P software v4.10 (Agilent Technologies, Inc.). The relative quantification of mRNA was performed using the comparative quantification cycle (Cq) method. The mRNA expression level was measured using the $2^{-\Delta\Delta Cq}$ method (22). The primer sequences used were as follows: Syk, forward 5'-CTCTGCCATTACCACTCCC-3' and reverse 5'-AGGTTC CAGGTCTGTTTCA-3'; caspase-1, forward 5'-TGCCTGGTC TTGTGACTTGGAG-3' and reverse 5'-ATGTCCTGGGAA

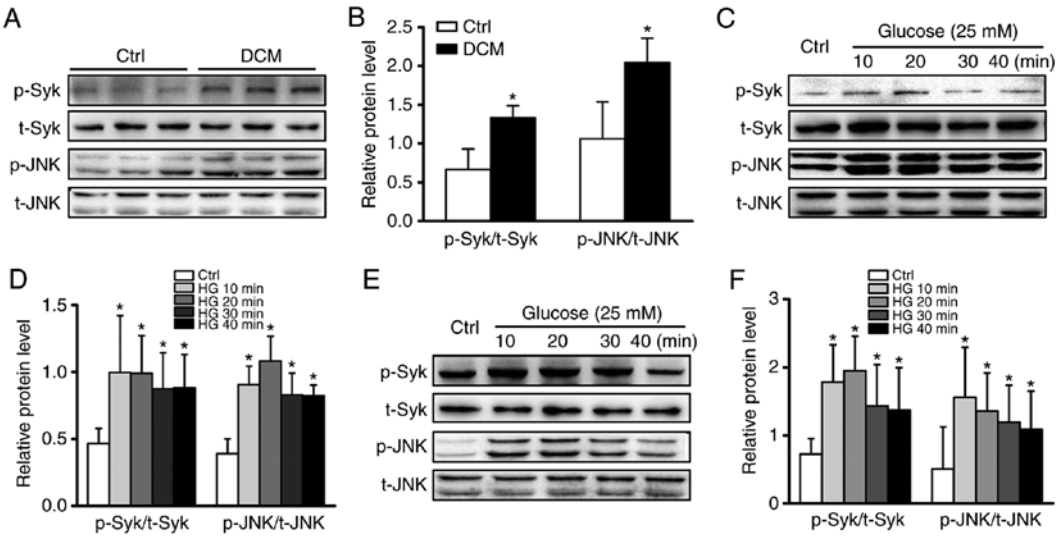

Figure 3. Phosphorylation of Syk and JNK in the hearts of DCM rats, HG-induced H9c2 cells and neonatal cardiomyocytes. (A) Total lysates from the myocardial tissue of rats in the control group at 12 weeks were extracted and subjected to western blotting to determine the phosphorylation levels of JNK and Syk. (B) Relative densitometric quantification analysis of the phosphorylation levels of JNK and Syk in A. (C) Protein expression levels of p-JNK and p-Syk in H9c2 cells cultured under 5.5 or 25.0 mM glucose conditions for 10, 20, 30 and 40 min. (D) Relative densitometric quantification analysis of the phosphorylation levels of JNK and Syk in C. (E) Protein expression levels of p-JNK and p-Syk in neonatal cardiomyocytes cultured under 5.5 or 25.0 mM glucose conditions for 10, 20, 30 and 40 min. (F) Relative densitometric quantification analysis of the phosphorylation levels of JNK and Syk in E. The data are presented as the mean ± standard error of the mean of three independent experiments. Statistical significance was determined by one-way analysis of variance followed by Tukey's post hoc test. *P<0.05, vs. 5.5 mM glucose. Ctrl, control; Syk, spleen tyrosine kinase; JNK, c-Jun N-terminal kinase; DCM, diabetic cardiomyopathy; HG, high glucose; p-, phosphorylated; t-, total.

GAGGTAGAAACG-3'; IL-1β, forward 5'-TGGGATGATGAC GACCTGC-3' and reverse 5'-GGAGAATACCACTTGTTG GCTTA-3'; GAPDH, forward 5'-GGGTGTGAACCACGA GAAAT-3' and reverse 5'-ACTGTGGTCATGAGCCCTTC-3'; The relative level of each gene was normalized to the level of GAPDH.

Syk-small interfering (si)RNA transfection. The H9c2 cells were transfected with Syk-siRNA (50 nM) using Lipofectamine™ 3000 (Thermo Fisher Scientific, Inc.), to knockdown Syk, following the manufacturer's protocol; a scramble siRNA, termed negative control (NC)-siRNA, was used as a control in the experiment. The sequences for rat Syk-siRNA were 5'-CCAGGUGGAAUAAUCUCAATT-3' (forward) and 5'-UUGAGAUUAUUCCACCUGGTT-3' (reverse). The sequences for the NC-siRNA were 5'-UUCUCC GAACGUGUCACGUTT-3' (forward) and 5'-ACGUGACAC GUUCGGAGAATT-3' (reverse). Following 48 h of transfection, the cells were treated with the HG and harvested for western blotting. The efficiency of Syk silencing was assessed by RT-qPCR analysis and western blotting.

Western blotting. The rat heart tissues were mechanically homogenized in lysis buffer (20 mM Tris HCl pH 8.0, 100 mM NaCl, 1 mM EDTA and 10% NP-40) supplemented with protease inhibitor (1:100 dilution, Sigma-Aldrich; Merck KGaA) and phosphatase inhibitor (1:100 dilution, Nanjing KeyGen Biotech Co., Ltd., Nanjing, China), and centrifuged (15,871 x g at 4˚C for 30 min) to remove cell debris. The proteins of the neonatal rat cardiomyocytes and H9c2 cells were prepared using RIPA buffer (cat. no. P0013B, Beyotime Institute of Biotechnology, Haimen, China) supplemented with protease and phosphatase inhibitors (1:100 dilution), and were centrifuged (15,871 x g at 4˚C for 30 min) to collect total proteins (supernatant). The total proteins were assessed using a BCA protein assay kit (Pierce; Thermo Fisher Scientific, Inc.) to measure the concentration. The protein samples from the rat heart tissues (80 g) or cardiomyocytes (40 g) were subjected to sodium dodecyl sulfate-polyacrylamide agarose gel electrophoresis in 10 or 12% gels and transferred electrophoretically onto a 0.22-mm polyvinylidene difluoride membrane (EMD Millipore, Billerica, MA, USA). Following blocking with 5% fat-free dry milk or BSA in Tris-buffered saline solution containing 0.05% Tween-20 for 2 h at room temperature, the membranes were incubated with the primary antibodies (listed above) overnight at 4˚C. Following three washes with Tris-buffered saline/Tween-20, the membranes were probed with secondary antibodies (anti-mouse IgG or anti-rabbit IgG) at room temperature for 1 h. The immunoreactive bands were visualized using enhanced chemiluminescent substrate (EMD Millipore). The density of bands was analyzed using Image J software 6.0 (National Institutes of Health, Bethesda, MD, USA).

Statistical analysis. All data are presented as the mean ± standard deviation of independent experiments. ImageJ Acquisition and Analysis software (version 6.0) was used to analyze the western blotting results. The statistical significances of differences between two groups were obtained using unpaired t-tests. One-way analysis of variance, followed by Dunnett's post hoc test, was used to compare between all columns and the control column. Tukey's post hoc test was used to compare all pairs of columns. Statistical analysis was performed using GraphPad Prism software (version 6.01; GraphPad Software, Inc., La Jolla, CA, USA). P<0.05 were considered to indicate a statistically significant difference.

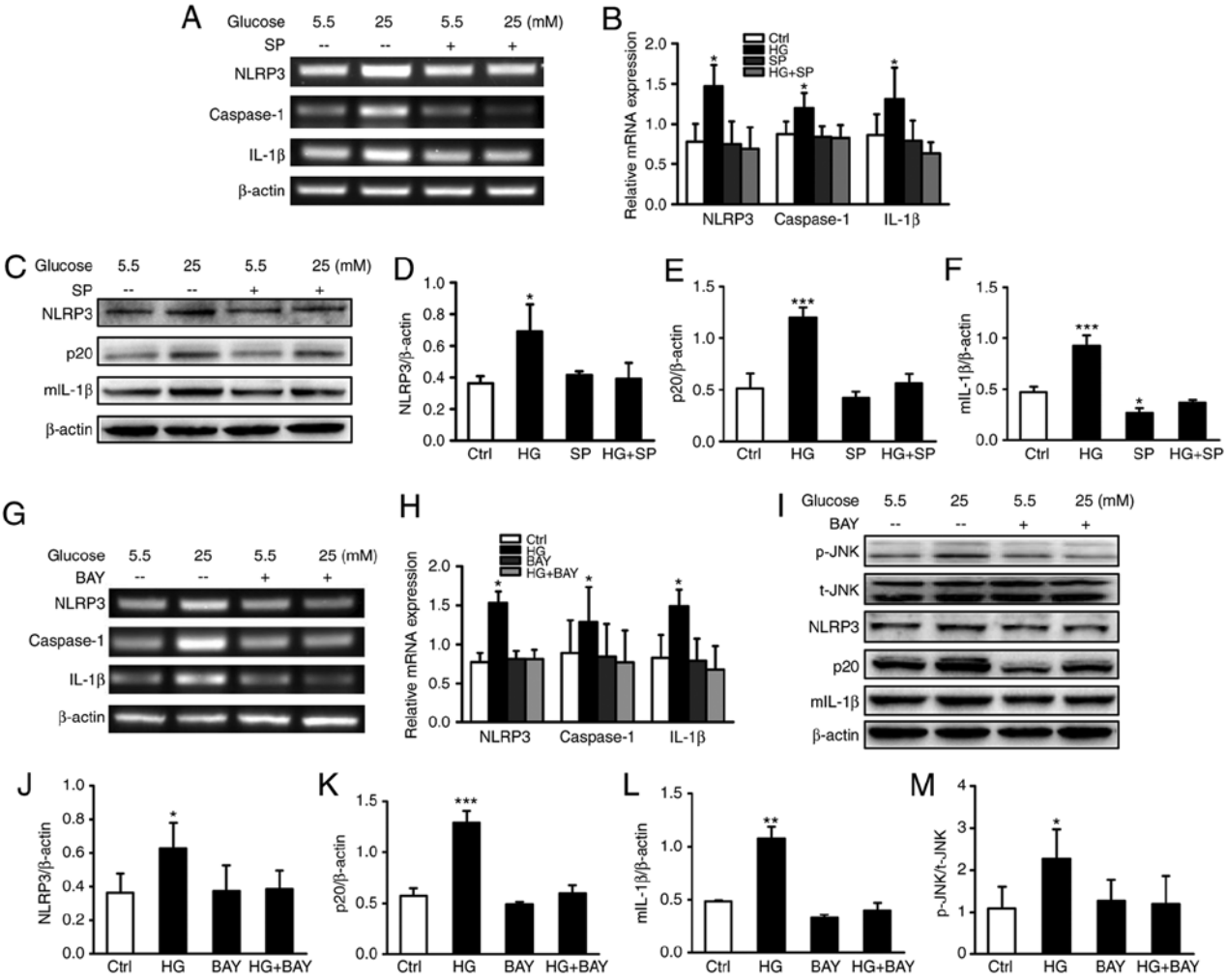

Figure 4. Inhibitors of JNK/Syk attenuate HG-induced NLRP3 inflammasome activation in H9c2 cells. (A) mRNA expression levels of NLRP3, caspase-1 and IL-1β were detected by RT-qPCR analysis following treatment with JNK inhibitor (10 μM) for 2 h in H9c2 cells. (B) Densitometric analysis of NLRP3, caspase-1 and IL-1β shown in A. (C) Protein expression levels of NLRP3, p20, mIL-1β and p-JNK of H9c2 cells were detected by western blotting following treatment with JNK inhibitor (10 μM) for 2 h and (D-F) densitometric analysis was performed in C. (G) mRNA expression levels of NLRP3, caspase-1 and IL-1β were detected by RT-qPCR analysis following treatment with Syk inhibitor (1 μM) for 2 h in in H9c2 cells. (H) Densitometric analysis of NLRP3, caspase-1 and IL-1β. (I) Protein expression levels of NLRP3, p20, mIL-1β and p-JNK in H9c2 cells were detected by western blotting following treatment with Syk inhibitor (1 μM) for 2 h and densitometric analysis of (J) NLRP3, (K) p20, (L) mIL-1β and (M) p-JNK was performed. The data are presented as the mean ± standard error of the mean of three independent experiments. Statistical significance was determined by one-way analysis of variance followed by Tukey's post hoc test. *P<0.05, **P<0.01 and ***P<0.001, vs. 5.5 mM glucose. Ctrl, control; JNK, c-Jun N-terminal kinase; Syk, spleen tyrosine kinase; NLRP3, NLR family pyrin domain-containing 3; HG, high glucose; IL, interleukin; RT-qPCR, reverse transcription-quantitative polymerase chain reaction; p-, phosphorylated; t-, total; mIL-1β, mature IL-1β; p20, caspase-1 p20; BAY, BAY61-3606.

Results

Characteristics of rats with STZ-induced DCM. The plasma blood glucose in the DCM rats was significantly increased (27.4±5 mM) when compared with that in the control group (6.5±0.6 mM) (Fig. 1A). The body weights were decreased in the DCM rats compared with those in the control group at the same point in time (Fig. 1B). Echocardiography showed that the E/A, FS% and EF% values of the diabetic rats at 12 weeks were significantly lower than those of the corresponding control group (Fig. 1C-E). In our previous study, cardiomyocyte hypertrophy was demonstrated using hematoxylin and eosin staining, and interstitial and perivascular fibrosis was demonstrated using Masson's trichrome staining in the heart of diabetic rats (21). Therefore, DCM characterized by systolic and diastolic dysfunction have been documented in diabetic rats.

NLRP3 inflammasome is activated in DCM rats, HG-induced H9c2 cells and neonatal cardiomyocytes. It has been reported that hyperglycemia may increase the expression of NLRP3 during diabetes and its complications. In the present study, it was found that the mRNA expression levels of NLRP3, caspase-1 and IL-1β were upregulated, peaking in the DCM rats at 12 weeks. In addition, the protein expression levels of NLRP3 at 12 weeks and its associated downstream molecules, including p20 and mIL-1β, at 16 weeks were considerably increased (data not shown). By contrast, no differences in the protein or mRNA expression levels of these molecules were observed in the control group in the different weeks (data not shown). Furthermore, the mRNA expression levels of NLRP3, caspase-1 and IL-1β in the heart tissues of three diabetic rats were significantly increased at 12 weeks, compared with those in the control group (Fig. 2A and B; P<0.05). As shown in

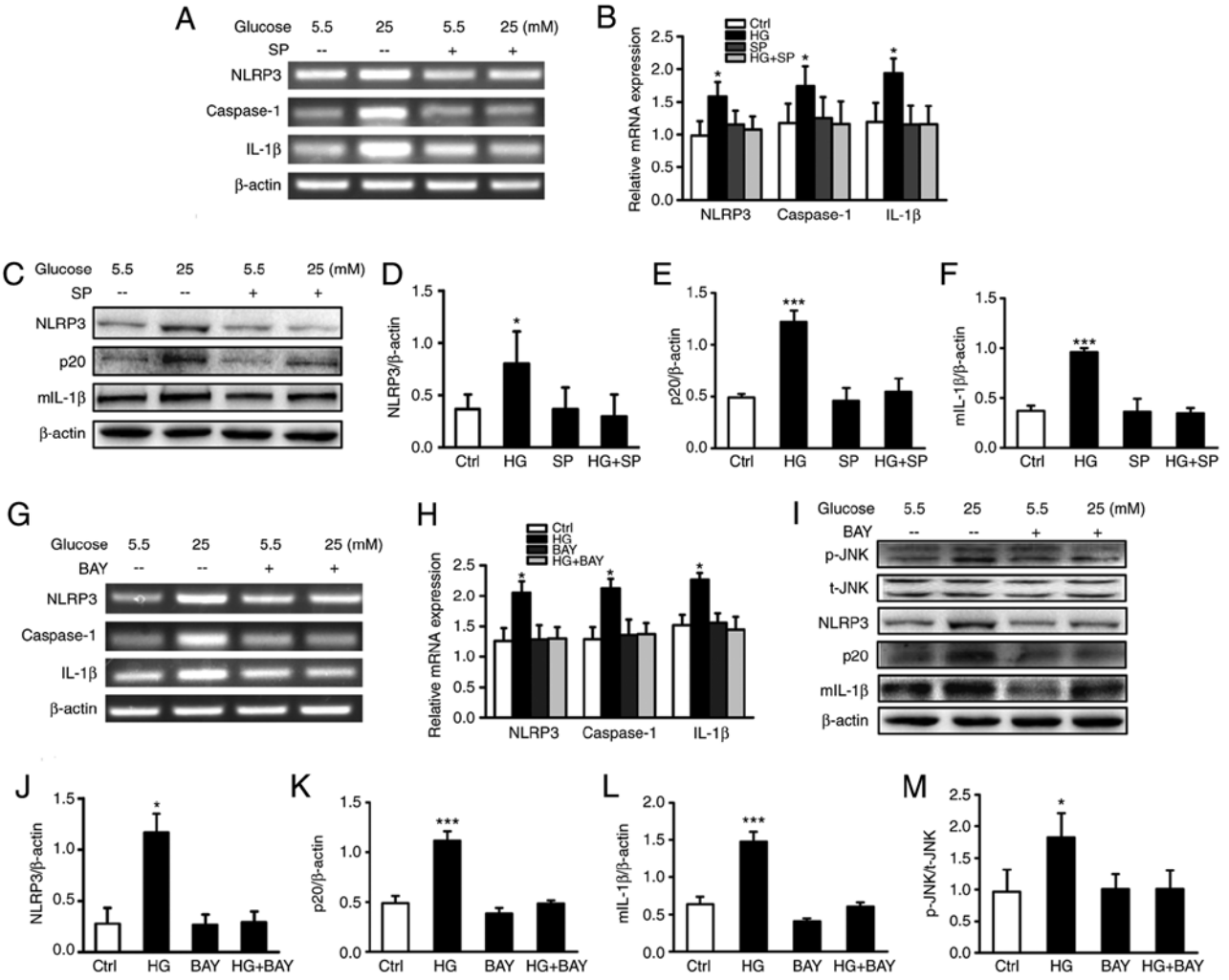

Figure 5. Inhibitors of JNK/Syk attenuate HG-induced NLRP3 inflammasome activation in neonatal cardiomyocytes. (A) mRNA expression levels of NLRP3, caspase-1 and IL-1β were detected by RT-qPCR analysis following treatment with JNK inhibitor (10 μM) for 2 h in neonatal cardiomyocytes. (B) Densitometric analysis of NLRP3, caspase-1 and IL-1β shown in A. (C) Protein expression levels of NLRP3, p20, mIL-1β and p-JNK of neonatal cardiomyocytes were detected by western blotting following treatment with JNK inhibitor (10 μM) for 2 h and (D-F) densitometric analysis was performed in C. (G) mRNA expression levels of NLRP3, caspase-1 and IL-1β were detected by RT-qPCR analysis following treatment with Syk inhibitor (1 μM) for 2 h in neonatal cardiomyocytes. (H) Densitometric analysis of NLRP3, caspase-1 and IL-1β. (I) Protein expression levels of NLRP3, p20, mIL-1β and p-JNK of neonatal cardiomyocytes were detected by western blotting following treatment with Syk inhibitor (1 μM) for 2 h and densitometric analysis of (J) NLRP3, (K) p20, (L) mIL-1β and (M) p-JNK was performed. Data are presented as the mean ± standard error of the mean of three independent experiments. Statistical significance was determined by one-way analysis of variance followed by Tukey's post hoc test. *P<0.05 and ***P<0.001, vs. 5.5 mM glucose. JNK, c-Jun N-terminal kinase; Syk, spleen tyrosine kinase; NLRP3, NLR family pyrin domain-containing 3; IL, interleukin; HG, high glucose; RT-qPCR, reverse transcription-quantitative polymerase chain reaction; p-, phosphorylated; t-, total; mIL-1β, mature IL-1β; p20, caspase-1 p20; SP, SP600125; BAY, BAY61-3606.

Fig. 2C-F, the protein expression levels of NLRP3 and p20, an active form of caspase-1, and mIL-1β in the heart tissues from three diabetic rats at 16 weeks were significantly higher than those from the control group (P<0.05, P<0.01 and P<0.01), indicating that the NLRP3 inflammasome was activated in the DCM rats.

Compared with cells treated with glucose at a concentration of 5.5 mM, the mRNA expression levels of NLRP3, caspase-1 and IL-1β were increased in the H9c2 cells and neonatal cardiomyocytes treated with 25.0 mM glucose (Fig. 2G-J; P<0.05). Simultaneously, the protein expression levels of NLRP3, p20 and mIL-1β, were markedly higher in the HG-induced H9c2 cells (Fig. 2K-N; P<0.05) and neonatal cardiomyocytes after 24 h (Fig. 2O-R; P<0.05). These data showed that the NLRP3 inflammasome was activated in cardiomyocytes under HG conditions.

Phosphorylation of Syk and JNK are increased in DCM rat hearts, HG-induced H9c2 cells and neonatal cardiomyocytes. Subsequently, it was revealed that the phosphorylation levels of JNK were increased in the diabetic rats at 12, 16, 20 and 33 weeks (data not shown), with levels in three 12-week-old DCM rats significantly increased, compared with the levels in the control rats (Fig. 3A and B; P<0.05). Of note, the phosphorylation levels of Syk in myocardial tissues from three 12-week-old DCM rats were significantly increased, compared with those from control rats (Fig. 3A and B; P<0.05). These results indicated that JNK and Syk may be involved in the pathogenesis of DCM.

Furthermore, it was found that the phosphorylation levels of Syk and JNK in the H9c2 cells (Fig. 3C and D; P<0.05) and neonatal cardiomyocytes under HG conditions (Fig. 3E and F; P<0.05) were increased in a time-dependent manner, peaking

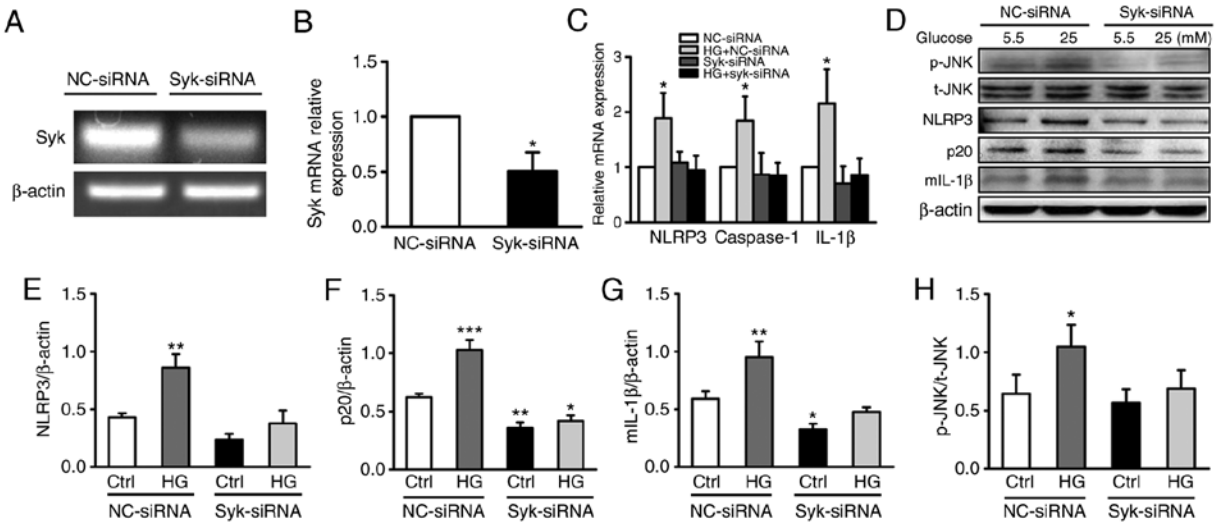

Figure 6. Syk serves a vital role in JNK-dependent NLRP3 inflammasome activation in HG-induced H9c2 cells and neonatal cardiomyocytes. (A) H9c2 cells were transfected for 48 h with either NC-siRNA or Syk-siRNA and (B) densitometric analysis was performed. (C) mRNA levels of NLRP3, caspase-1 and IL-1β were measured by reverse transcription-quantitative polymerase chain reaction analysis. (D) H9c2 cells transfected with siRNA against Syk were exposed to HG conditions for 48 h and the protein expression levels of p-JNK, NLRP3, p20 and mIL-1β were measured by western blotting; densitometry of (E) NLRP3, (F) p20, (G) mIL-1β and (H) p-JNK was performed using Image J software. Data are presented as the mean ± standard error of the mean of three independent experiments. Statistical significance was determined by one-way analysis of variance followed by Tukey's post hoc test. *P<0.05, **P<0.01 and ***P<0.001, vs. 5.5 mM glucose. Syk, spleen tyrosine kinase; JNK, c-Jun N-terminal kinase; NLRP3, NLR family pyrin domain-containing 3; NC, negative control; siRNA, small interfering RNA; Ctrl, control; HG, high glucose; p, phosphorylated; p20, caspase-1 p20; mIL-1β, mature interleukin 1β.

at 20 min. By contrast, high osmolarity had no effect on the phosphorylation level of Syk or JNK in H9c2 cells or neonatal cardiomyocytes (Fig. S1A-D). These data revealed that Syk and JNK were considerably activated in HG-induced neonatal cardiomyocytes.

Inhibitors of JNK attenuate HG-induced NLRP3 inflammasome activation in H9c2 cells and neonatal cardiomyocytes. The results of the mRNA and protein expression analyses are shown in Figs. 4 and 5. The JNK inhibitor attenuated the HG-induced increased mRNA expression of NLRP3, caspase-1 and IL-1β in H9c2 cells (Fig. 4A and B) and neonatal cardiomyocytes (Fig. 5A and B). Similarly, the protein expression levels of NLRP3, p20 and mIL-1β were downregulated in the H9c2 cells (Fig. 4C-F) and neonatal cardiomyocytes (Fig. 5C-F) following JNK inhibitor treatment subsequent to HG induction. These data indicated that JNK may serve a critical role in NLRP3 inflammasome activation, leading to the maturation of IL-1β.

Syk is vital in JNK-dependent NLRP3 inflammasome activation in HG-induced H9c2 cells and neonatal cardiomyocytes. Subsequently, the present study investigated whether Syk was involved in HG-induced JNK-dependent NLRP3 inflammasome activation in diabetic cardiopathy. As shown in Figs. 4I-M and 5I-M, the HG-induced phosphorylation of JNK was significantly reduced following Syk inhibitor treatment in the H9c2 cells and neonatal cardiomyocytes. The HG-induced mRNA expression levels of NLRP3, caspase-1 and IL-1β (Figs. 4G, H and 5G, H) and the protein expression levels of NLRP3, p20 and mIL-1β (Figs. 4I-L and 5I-L) were also decreased, indicating that Syk may be involved in JNK-dependent NLRP3 inflammasome activation in H9c2 cells and neonatal cardiomyocytes exposed to HG.

In order to further confirm whether Syk promoted JNK-dependent NLRP3 inflammasome activation in cardiomyocytes under HG conditions, the H9c2 cells were transfected with Syk-siRNA. The silencing efficiency of the Syk-siRNA sequence reached 55% via RT-qPCR (Fig. 6A and B). It was observed that the mRNA levels of JNK-dependent NLRP3, caspase-1 and IL-1β (Fig. 6C), and the protein levels of NLRP3, p20 and mIL-1β were markedly reduced in the HG-induced H9c2 cells by Syk-siRNA (Fig. 6D-G). The HG-induced phosphorylation of JNK was also significantly downregulated by Syk-siRNA (Fig. 6D and H). These data suggested that Syk serves a vital role in JNK-dependent NLRP3 inflammasome activation, leading to the maturation of IL-1 in HG-induced H9c2 cells and neonatal cardiomyocytes.

Discussion

Diabetes is a pro-inflammatory state, and a previous review reported an increased concentration of cytokines, including TNF-α and IL-6, in the myocardial tissue of various mouse models of diabetes (23), implicating inflammation in the development of DCM. In the present study, it was found that the expression of the NLRP3 inflammasome was markedly increased, leading to the maturation of IL-1β in DCM rats, HG-induced neonatal cardiomyocytes and H9c2 cells. This indicates the involvement of the NLRP3 inflammasome-dependent activation of caspase-1 in the subsequent maturation of IL-1β during DCM. It has been reported that hyperglycemia may promote the expression of several inflammatory cytokines in rat H9c2 cells (24), including IL-1β, a vital pro-inflammatory cytokine that can lead to persistent inflammation in the myocardium, resulting in diabetic cardiac dysfunction (8). The expression of IL-1β is gradually elevated during glucose tolerance injury in type 2 DM, and is posi-

tively correlated with insulin resistance (25). Furthermore, the maturation and secretion of IL-1β is mainly controlled by the activation of caspase-1 through the NLRP3 inflammasome, which is composed of NLRP3, apoptosis-associated speck-like protein containing a CARD and pro-caspase-1 (26). Of note, in the present study, the cardiac expression of NLRP3 in the DCM rats peaked at 12 weeks, and then decreased in a time-dependent manner. In combination with the results of the aforementioned studies, it was concluded that NLRP3 inflammasome-mediated inflammation is involved in the early stage progression of DCM.

However, the specific mechanisms leading to NLRP3 inflammasome activation remain to be fully elucidated. In the present study, the expression of p-JNK was markedly increased in DCM rat hearts and HG-induced cardiomyocytes. Consistently, a previous study reported that the p-JNK pathway was activated by reactive oxygen species (ROS) in HG conditions (27,28). By contrast, inhibition of the phosphorylation of JNK or mitochondrial oxidative damage can reduce myocardial fibrosis (29) and myocardial cell injury (30). In the present study, the inhibition of JNK significantly decreased the expression of NLRP3 at the mRNA and protein levels. Its downstream molecules, including p20 and mIL-1β, were also significantly reduced. These results indicated that JNK was required for HG-induced NLRP3 inflammasome activation in cardiomyocytes.

As limited investigations have been performed on the role of Syk in HG-induced intracellular signal transduction, the specific role of Syk in the development of DCM remains to be fully elucidated. It was demonstrated herein that the phosphorylation level of Syk was markedly increased in the DCM rat hearts, compared with that in the control rat hearts. Of note, these changes were reversed by Syk-siRNA transfection and Syk inhibitor treatment *in vitro*, suggesting the involvement of Syk in cardiomyopathy. A recent study by Zhou *et al* (31) reported that Syk was activated by chronic HG stimulation in DCM, consistent with our previous conclusion (32). The results of the above studies suggest that Syk is involved in DCM. It was also found that Syk-siRNA transfection and Syk inhibitor treatment reduced JNK-dependent NLRP3 inflammasome activation in the HG-induced myocardial cells. In addition, our previous study reported that Syk was involved in the regulation of HG stimulation-induced cardiomyocyte apoptosis (33). It is concluded for the first time, to the best of our knowledge, that the Syk-mediated JNK signaling pathway promoted activation of the NLRP3 inflammasome, leading to the maturation of IL-1 and myocardial cell injury caused by Syk-mediated apoptosis during the development of DCM.

Previous studies have revealed that the inflammatory caspase family cleaves the protein gasdermin D (GSDMD) to trigger a caspase-1-dependent form of regulated cell death, known as pyroptosis (34,35). NF-κB can elevate the transcription of GSDMD by binding to two proximal binding sites upstream of the GSDMD promoter region (36). Kuo *et al* (18) found that HG led to an increase in ROS levels and activated the JNK/NF-κB signaling pathway in H9c2 cardiomyoblasts and neonatal cardiomyocytes. Therefore, GSDMD-mediated pyroptosis may be involved in the pathogenesis of DCM, the underlying mechanism of which requires investigation.

In conclusion, it was demonstrated in the present study that Syk was markedly activated in the development of DCM, subsequently promoting NLRP3 inflammasome activation through the phosphorylation of JNK, leading to the cleavage of pro-caspase-1 and maturation of IL-1β, and finally contributing to diabetic cardiac dysfunction. These results suggest that Syk may be a potential target for the treatment of patients with DCM. However, the present study had several limitations. First, due to the lack of Syk-knockout or inhibitor-treated animal models, the associations among JNK, Syk and NLRP3 were investigated in cardiomyocytes only *in vitro*, and therefore the results cannot be extrapolated *in vivo*. Second, additional investigations are required to determine how HG promotes the phosphorylation of Syk in cardiomyocytes. Finally, further investigations are also required to examine the specific mechanistic link between the modulation of JNK and/or Syk and NLRP3 inflammasome activation.

Acknowledgements

Not applicable.

Funding

This study was supported by the National Basic Research Program of China (973 Program; grant no. 2015CB553605), the National Natural Science Foundation of China (grant nos. 81772252, 31400762 and 81200116) and the Key Laboratory of Myocardial Ischemia, Harbin Medical University, Chinese Ministry of Education (grant no. KF201303).

Availability of data and materials

All data generated or analyzed during this study are included in this published article, and more detailed data obtained during the present study are available from the corresponding author on reasonable request.

Authors' contributions

SL, RL and MX contributed equally to the present study, and were involved in the research, acquisition and analysis of the data. SL, RL, MX, YQ, YCh and GL were involved in data acquisition. YCu and YS contributed to the conception and design of the study. XT, YH and PZ were involved in the analysis and interpretation of data. XD and ZQ were involved in manuscript drafting, revising and final approval of the version to be submitted. YCu and YS contributed to the funding application. All authors read and approved the final manuscript.

Ethics approval and consent to participate

All animal experimental procedures performed in the present study were approved by the Animal Care and Welfare Committee of Tianjin Medical University (Tianjin, China; date of application, 10th January 2017; approval no. TMuaMEC2017027).

Patient consent for publication

Not applicable.

Competing interests

The authors declare that they have no competing interests.

References

1. Whiting DR, Guariguata L, Weil C and Shaw J: IDF diabetes atlas: Global estimates of the prevalence of diabetes for 2011 and 2030. Diabetes Res Clin Pract 94: 311-321, 2011.
2. Thrainsdottir IS, Aspelund T, Thorgeirsson G, Gudnason V, Hardarson T, Malmberg K, Sigurdsson G and Rydén L: The association between glucose abnormalities and heart failure in the population-based Reykjavik study. Diabetes Care 28: 612-616, 2005.
3. Redfield MM, Jacobsen SJ, Burnett JC Jr, Mahoney DW, Bailey KR and Rodeheffer RJ: Burden of systolic and diastolic ventricular dysfunction in the community: Appreciating the scope of the heart failure epidemic. JAMA 289: 194-202, 2003.
4. Marcinkiewicz A, Ostrowski S and Drzewoski J: Can the onset of heart failure be delayed by treating diabetic cardiomyopathy? Diabetol Metab Syndr 9: 21, 2017.
5. Zhang X, Pan L, Yang K, Fu Y, Liu Y, Chi J, Zhang X, Hong S, Ma X and Yin X: H3 relaxin protects against myocardial injury in experimental diabetic cardiomyopathy by inhibiting myocardial apoptosis, fibrosis and inflammation. Cell Physiol Biochem 43: 1311-1324, 2017.
6. Abdel-Hamid AA and Firgany Ael-D: Atorvastatin alleviates experimental diabetic cardiomyopathy by suppressing apoptosis and oxidative stress. J Mol Histol 46: 337-345, 2015.
7. Niu J, Gilliland MG, Jin Z, Kolattukudy PE and Hoffman WH: MCP-1and IL-1β expression in the myocardia of two young patients with Type 1 diabetes mellitus and fatal diabetic ketoacidosis. Exp Mol Pathol 96: 71-79, 2014.
8. Liu Z, Zhao N, Zhu H, Zhu S, Pan S, Xu J, Zhang X, Zhang Y and Wang J: Circulating interleukin-1β promotes endoplasmic reticulum stress-induced myocytes apoptosis in diabetic cardiomyopathy via interleukin-1 receptor-associated kinase-2. Cardiovasc Diabetol 14: 125, 2015.
9. Westermann D, Rutschow S, Jäger S, Linderer A, Anker S, Riad A, Unger T, Schultheiss HP, Pauschinger M and Tschöpe C: Contributions of inflammation and cardiac matrix metalloproteinase activity to cardiac failure in diabetic cardiomyopathy: The role of angiotensin type 1 receptor antagonism. Diabetes 56: 641-646, 2007.
10. Zhang X, Fu Y, Li H, Shen L, Chang Q, Pan L, Hong S and Yin X: H3 relaxin inhibits the collagen synthesis via ROS and P2X7R-mediated NLRP3 inflammasome activation in cardiac fibroblasts under high glucose. J Cell Mol Med 22: 1816-1825, 2018.
11. Lee HM, Kim JJ, Kim HJ, Shong M, Ku BJ and Jo EK: Upregulated NLRP3 inflammasome activation in patients with type 2 diabetes. Diabetes 62: 194-204, 2013.
12. Wang C, Pan Y, Zhang QY, Wang FM and Kong LD: Quercetin and allopurinol ameliorate kidney injury in STZ-treated rats with regulation of renal NLRP3 inflammasome activation and lipid accumulation. PLoS One 7: e38285, 2012.
13. Lebreton F, Berishvili E, Parnaud G, Rouget C, Bosco D, Berney T and Lavallard V: NLRP3 inflammasome is expressed and regulated in human islets. Cell Death Dis 9: 726, 2018.
14. Luo B, Huang F, Liu Y, Liang Y, Wei Z, Ke H, Zeng Z, Huang W and He Y: NLRP3 inflammasome as a molecular marker in diabetic cardiomyopathy. Front Physiol 8: 519, 2017.
15. Geahlen RL: Getting Syk: Spleen tyrosine kinase as a therapeutic target. Trends Pharmacol Sci 35: 414-422, 2014.
16. Javadov S, Jang S and Agostini B: Crosstalk between mitogen-activated protein kinases and mitochondria in cardiac diseases: Therapeutic perspectives. Pharmacol Ther 144: 202-225, 2014.
17. Han MS, Jung DY, Morel C, Lakhani SA, Kim JK, Flavell RA and Davis RJ: JNK expression by macrophages promotes obesity-induced insulin resistance and inflammation. Science 339: 218-222, 2013.
18. Kuo WW, Wang WJ, Tsai CY, Way CL, Hsu HH and Chen LM: Diallyl trisufide (DATS) suppresses high glucose-induced cardiomyocyte apoptosis by inhibiting JNK/NFκB signaling via attenuating ROS generation. Int J Cardiol 168: 270-280, 2013.
19. Watanabe N, Shikata K, Shikata Y, Sarai K, Omori K, Kodera R, Sato C, Wada J and Makino H: Involvement of MAPKs in ICAM-1 expression in glomerular endothelial cells in diabetic nephropathy. Acta Med Okayama 65: 247-257, 2011.
20. Yang WS, Chang JW, Han NJ, Lee SK and Park SK: Spleen tyrosine kinase mediates high glucose-induced transforming growth factor-β1 up-regulation in proximal tubular epithelial cells. Exp Cell Res 318: 1867-1876, 2012.
21. Pang A, Hu Y, Zhou P, Long G, Tian X, Men L, Shen Y, Liu Y and Cui Y: Corin is down-regulated and exerts cardioprotective action via activating pro-atrial natriuretic peptide pathway in diabetic cardiomyopathy. Cardiovasc Diabetol 14: 134, 2015.
22. Livak KJ and Schmittgen TD: Analysis of relative gene expression data using real-time quantitative PCR and the 2(-Delta Delta C(T)) method. Methods 25: 402-408, 2001.
23. Diamant M, Lamb HJ, Smit JW, de Roos A and Heine RJ: Diabetic cardiomyopathy in uncomplicated type 2 diabetes is associated with the metabolic syndrome and systemic inflammation. Diabetologia 48: 1669-1670, 2005.
24. Pan Y, Wang Y, Zhao Y, Peng K, Li W, Wang Y, Zhang J, Zhou S, Liu Q, Li X, *et al*: Inhibition of JNK phosphorylation by a novel curcumin analog prevents high glucose-induced inflammation and apoptosis in cardiomyocytes and the development of diabetic cardiomyopathy. Diabetes 63: 3497-3511, 2014.
25. Sun X, Hao H, Han Q, Song X, Liu J, Dong L, Han W and Mu Y: Human umbilical cord-derived mesenchymal stem cells ameliorate insulin resistance by suppressing NLRP3 inflammasome-mediated inflammation in type 2 diabetes rats. Stem Cell Res Ther 8: 241, 2017.
26. Youm YH, Adijiang A, Vandanmagsar B, Burk D, Ravussin A and Dixit VD: Elimination of the NLRP3-ASC inflammasome protects against chronic obesity-induced pancreatic damage. Endocrinology 152: 4039-4045, 2011.
27. Wang C, Zou S, Cui Z, Guo P, Meng Q, Shi X, Gao Y, Yang G and Han Z: Zerumbone protects INS-1 rat pancreatic beta cells from high glucose-induced apoptosis through generation of reactive oxygen species. Biochem Biophys Res Commun 460: 205-209, 2015.
28. Chen J, Mo H, Guo R, You Q, Huang R and Wu K: Inhibition of the leptin-induced activation of the p38 MAPK pathway contributes to the protective effects of naringin against high glucose induced injury in H9c2 cardiac cells. Int J Mol Med 33: 605-612, 2014.
29. Yu Y, Jia XJ, Zhang WP, Fang TT, Hu J, Ma SF and Gao Q: The protective effect of low-dose Ethanol on myocardial fibrosis through downregulating the JNK signaling pathway in diabetic rats. J Diabetes Res 2016: 3834283, 2016.
30. Yan X, Xun M, Li J, Wu L, Dou X and Zheng J: Activation of Na^+/K^+-ATPase attenuates high glucose-induced H9c2 cell apoptosis via suppressing ROS accumulation and MAPKs activities by DRm217. Acta Biochim Biophys Sin (Shanghai) 48: 883-893, 2016.
31. Zhou H, Yue Y, Wang J, Ma Q and Chen Y: Melatonin therapy for diabetic cardiomyopathy: A mechanism involving Syk-mitochondrial complex I-SERCA pathway. Cell Signal 47: 88-100, 2018.
32. Chen YF, Long GF, Tian XX, Qiao YC, Li SY, Xue MT, Liu YD, Cui YJ and Shen YN: Studies on the mechanism of Syk and JNK in the heart tissue of type 1 diabetic rats. Tianjin Med J 45: 463-467, 2017 (In Chinese).
33. Long G, Xue M, Cheb Y, Qiao Y, Tian X, Li S, Liu Y, Shen Y and Cui Y: Effects of Syk on regulation of high glucose-induced apoptosis of H9c2 myocardial cells and its mechanism. Int J Endocrinol Metabolism 37: 303-307, 2017.
34. Shi J, Zhao Y, Wang K, Shi X, Wang Y, Huang H, Zhuang Y, Cai T, Wang F and Shao F: Cleavage of GSDMD by inflammatory caspases determines pyroptotic cell death. Nature 526: 660-665, 2015.
35. Kovacs SB and Miao EA: Gasdermins: Effectors of pyroptosis. Trends Cell Biol 27: 673-684, 2017.
36. Liu Z, Gan L, Xu Y, Luo D, Ren Q, Wu S and Sun C: Melatonin alleviates inflammasome-induced pyroptosis through inhibiting NF-κB/GSDMD signal in mice adipose tissue. J Pineal Res 63, 2017.